Phase Stability of Polyelectrolyte Solutions As Predicted from Lattice Mean-Field Theory

Michael Gottschalk,† Per Linse,* and Lennart Piculell

Physical Chemistry 1, Center for Chemistry and Chemical Engineering, Lund University, P.O. Box 124, S-221 00 Lund, Sweden

Received June 2, 1998; Revised Manuscript Received August 25, 1998

ABSTRACT: An extension of the Flory−Huggins lattice theory to include charged polymers is described and utilized to predict the polymer solubility in solvent/polymer and solvent/polymer/salt systems and the polymer miscibility in solvent/polymer 1/polymer 2 systems. In the extended theory, all simple ions (counterions to the polymer and ions from the salt) are treated on the same level as the other components and the effect of the electrostatic interaction is included by imposing electroneutral phases. It was found that charging the polymer generally increases the polymer solvency or polymer miscibility. In those cases where both polymers carry charges of the same sign, the minimal miscibility is obtained at such conditions that the coexisting phases have similar counterion concentration. Generally, the increased solubility/miscibility could be attributed to the contribution from the mixing entropy of the small ions. Good qualitative agreement with several experimental investigations are found. The increased solubility of alkoxy polymers in aqueous solution upon an introduction of charged groups is also investigated.

Introduction

The introduction of charges on a water-insoluble polymer generally increases its solubility in water. Similarly, the introduction of charges on one of the two polymers in an aqueous polymer mixture increases the miscibility of the two polymers.[1,2] Added salt reduces the effects of the charges. For ternary solvent/polymer/polymer systems an introduction of charges of the same sign on both polymers reduces the favorable miscibility effect seen when charging only one of the polymers.[3−5] These observations indicate that the mixing entropy of the small counterions of the polyelectrolytes plays an important role for the solubility and for the miscibility in polyelectrolyte systems, and they have inspired theoretical investigations on the Flory−Huggins level of the solubility and miscibility of polyelectrolyte solutions. Khokhlov and Nyrkova[6] have shown that the mixing entropy of the counterions could be dealt with within the standard Flory−Huggins theory by a renormalization of the number of polymer segments. Independently, Nilsson[4,7] and later Johansson et al.[8] numerically solved models based on an extended version of the Flory−Huggins theory, where the counterions were explicitly included as a separate component on the same level as the solvent and the chain molecules. In the spirit of the random-mixing approximation, the charges of each component in a phase are uniformly distributed, leading to zero electrostatic energy and the effect of the electrostatic interactions among the charges enters the model only by imposing that each phase should be electroneutral. Both approaches predict results in qualitative agreement with experimental data.[4,6]

Ternary solvent/polymer/surfactant systems also display segregative phase behavior similar to those of ternary solvent/polymer/polymer systems.[7,9] The explanation for this similarity is the lower mixing entropy possessed by the surfactants molecules when being in the micellar state. Polymer-like phase behavior of this kind was found also for slightly charged aqueous mixtures of sodium dextran sulfate with penta(ethylene oxide) dodecyl ether + sodium dodecyl sulfate.[5] The use of one uncharged and one charged type of surfactant molecules offered the possibility of a continuous regulation of the micellar charge.

In this contribution we extend the investigations of the phase behavior of binary and ternary polyelectrolyte systems, and we have included systems where polymers possess internal states (the role of the internal state will be discussed below). In the theoretical section we give an account of the extension of the Flory−Huggins theory adapted for copolymers with internal states to charged polymer systems by employing the approach taken by Nilsson.[4,7] We also provide a comparison with the approach taken by Khokhlov and Nyrkova.[6] Then we present results from binary solvent/polymer solutions and how the two-phase boundaries are affected by the introduction of charges on the polymer and by the addition of salt. Thereafter, we investigate the effects of introducing charges on one or both of the polymers in a ternary solvent/polymer/polymer system and make qualitative comparison with experimental data. For both the binary and the ternary systems we compare some of our predictions with those obtained from the approach made by Khokhlov and Nyrkova. Finally, we examine the charge effects in a more sophisticated polymer model where the polymers possess internal states as developed by Karlström.[10] Such an approach has shown to be very fruitful for systems containing poly(ethylene oxide) (PEO), polyl(propylene oxide) (PPO), and related polymers, which display a reduced solubility in aqueous solution upon a temperature increase, see, for example, refs 11−13. The results are hence predictions of the phase behavior of charged alkoxy polymers in aqueous solution. The paper ends with a summary.

* To whom correspondence should be addressed.
† Present address: Physical Chemistry 2, Center for Chemistry and Chemical Engineering, Lund University, P.O. Box 124, S-221 00 Lund, Sweden.

10.1021/ma980866d CCC: $15.00
Published on Web 10/28/1998

Theoretical Concepts

The Flory−Huggins lattice theory[14] for homogeneous solutions of homopolymers has previously been extended to solutions of polyelectrolytes[4,6] and to systems containing homopolymers possessing internal states,[10] which later was generalized to copolymers.[15] We will in the following combine the extensions made by Nilsson[4] and by Linse and Björling[15] to obtain a theory capable of modeling charged copolymers having internal states. Moreover, we will relate the free energy expression for the case of charged homopolymers to that given by Khokhlov and Nyrkova.[6]

Free Energy Expressions. The basis of the calculations of phase diagrams is the expression of the mixing free energy. For a multicomponent system consisting of *un*charged components [solvent(s) and polymer(s) with internal states], the Helmholtz free energy of mixing becomes[15]

$$\beta(A - A^*) = \beta(A_{\text{int}} - A^*_{\text{int}}) - \ln\frac{\Omega}{\Omega^*} + \beta(U - U^*) \quad (1)$$

where A_{int} represents the internal energy arising from the internal states in the mixed system, A^*_{int} the internal energy in the reference system (where the components are in pure amorphous states), $\ln(\Omega/\Omega^*)$ the mixing configurational entropy divided by the Boltzmann constant, U and U^* the configurational energy in the mixed and reference system, respectively, and $\beta = 1/(kT)$, with k being Boltzmann's constant and T the absolute temperature. In the general case of a system with copolymers, the internal free energy, the mixing configurational entropy, and the interaction energy of the mixed system can be expressed as[15]

$$\beta A_{\text{int}} = \sum_x \sum_A n_x r_{Ax} \sum_B P_{AB}\left[\beta U_{AB} + \ln\frac{P_{AB}}{g_{AB}}\right]$$

$$\ln\frac{\Omega}{\Omega^*} = -\sum_x n_x \ln\frac{n_x r_x}{L} \quad (2)$$

$$\beta U = \frac{1}{2}\sum_x \sum_A \sum_{A'} \sum_B \sum_{B'} n_x r_{Ax} P_{AB}\, \chi_{BB'} P_{A'B'} \phi_{A'}$$

where n_x denotes the total number of molecules of type x, r_{Ax} the number of segments of type A in component x, r_x the total number of segments in component x ($r_x = \Sigma_A r_{Ax}$), L the total number of lattice sites ($L = \Sigma_x n_x r_x$), ϕ_A the volume fraction of species A [$\phi_A = (1/L)\Sigma_x n_x r_{Ax}$], and $\chi_{BB'}$ the Flory−Huggins interaction parameter between species A in state B and species A' in state B'. Moreover, P_{AB} is the fraction of species A in state B, U_{AB} the internal energy of species A in state B, and g_{AB} the degeneration of species A in state B. The state distribution at equilibrium (i.e., the fraction of species A being in state B at equilibrium) is obtained by minimizing $A - A^*$ with respect to $\{P_{AB}\}$ subjected to the constraint $\Sigma_B P_{AB} = 1$, for all A, which gives

$$P_{AB} = \frac{g_{AB}\exp[-\beta U_{AB} - \sum_{A'}\sum_{B'} \chi_{BB'} P_{A'B'}\phi_{A'}]}{\sum_B g_{AB}\exp[-\beta U_{AB} - \sum_{A'}\sum_{B'} \chi_{BB'} P_{A'B'}\phi_{A'}]} \quad (3)$$

For the simplified case of a system consisting of solvent(s) and homopolymer(s) without internal states, the mixing free energy is reduced to

$$\beta(A - A^*) = L\sum_x \frac{\phi_x}{r_x}\ln\phi_x + \frac{L}{2}\sum_x\sum_{x'}\phi_x\chi_{xx'}\phi_{x'} \quad (4)$$

where r_x and L have the same meaning as above and where ϕ_x denotes the volume fraction of component x [$\phi_x = n_x r_x/L$] and $\chi_{xx'}$ the Flory−Huggins interaction parameter between a segment in component x and a segment in component x'. The summation extends over all components in the system. Finally, for a binary solution, we retrieve from eq 4 the well-known free energy expression $\beta(A - A^*)/L = (\phi_1/r_1)\ln\phi_1 + (\phi_2/r_2)\ln\phi_2 + \phi_1\chi_{12}\phi_2$.[14]

So far, the theory is applicable to uncharged components. The extension of the homogeneous lattice theory to charged components (with or without internal states) involves the following: (i) the description of the polymers remains the same except that they carry charges, (ii) the counterions of the polyelectrolyte(s) and small ions from simple salt are introduced as additional and separate components, and (iii) the effects of the electrostatic interaction are taken into account by requiring each macroscopic phase to be electroneutral.

Hence, eqs 1−3 (for the case of copolymers with internal states) or (eq 4 for the case of homopolymers without internal states) remain the same, except that the summations now also involve the small ions (counterions and small ions arising from simple salt) as well. Moreover, we require that each macroscopic phase has to be electroneutral, and thus there is no explicit energy term describing the electrostatic interaction.

In the present work, the solvent and the small ions occupy one lattice site each, $r = 1$, whereas for the polymers, $r > 1$. For simplicity, all interaction parameters involving the small ions are here set to zero.

Calculation of Phase Diagrams. Given the overall composition of the system $\{n_x\}$, the equilibrium is achieved when $\{n_x\}$ is distributed among the coexisting phases $\{\alpha\}$ such that the total free energy

$$A_{\text{tot}} = \sum_\alpha A_\alpha(\{n_x{}^\alpha\}) \quad (5)$$

where $A^\alpha(\{n_x{}^\alpha\})$ is given by eqs 1−3, or by eq 4, attains its global minimum subjected to the mass conservation constraint:

$$n_x = \sum_\alpha n_x{}^\alpha \quad (6)$$

for all x. In the presence of charged components, we require an additional charge neutrality of all phases. For copolymers, where we allow the different states to carry different fractional charges, we have the constraint

$$0 = \sum_x\sum_A\sum_B \tau_{AB} P_{AB}{}^\alpha r_{Ax} n_x{}^\alpha \quad (7)$$

where τ_{AB} denotes the fractional charge (including sign) of species A in state B and $P_{AB}{}^\alpha$ the fraction of species A being in state B in phase α. For homopolymers without internal states, eq 7 reduces to

$$0 = \sum_x \tau_x r_x n_x{}^\alpha \quad (7')$$

where τ_x denotes the fractional elementary charge (including sign) per segment of component x.

Numerical Procedure. In practice, the minimization of A_{tot} subjected to the constraints given by eqs 6 and 7 is performed by an iterative process. The different molecules are distributed randomly among N solutions, where N is the number of independent components. The total free energy A_{tot} is minimized by repetitive movements of a given amount of the different components among the N solutions in a systematic manner. Only those moves where the free energy is reduced are accepted. When no further moves are accepted, the amount to be moved is reduced and the process is repeated again. Finally, when the change in A_{tot} becomes sufficiently small, the iteration is halted. By examination of the compositions of the N solutions, the number of coexisting phases is established. Solutions with the same composition (within a given tolerance) are regarded as belonging to the same phase. In the iteration procedure, the charge neutrality condition is introduced by adding a free energy penalty proportional to the square of the deviation from electroneutrality. For good convergence, the prefactor should increase as the iteration proceeds. Throughout, the state distribution is determined by using eq 3 iteratively each time the composition of any solution is changed.

The described procedure does not guarantee that the global minimum is achieved. However, when different initial distributions of the components were used, we have in all cases obtained the same numerical solution, and the numerical solutions have been well-behaved as the initial conditions were slightly changed, supporting that we have obtained the global free energy minimum.

Relation to the Approach by Khokhlov and Nyrkova. As will be obvious from the results, the increased solubility of polyelectrolytes as compared to that of the corresponding polymers arises from the mixing entropy of the counterions of the polyelectrolyte. On the basis of this insight, Khokhlov and Nyrkova mapped the model of a polyelectrolyte solution onto a model of a polymer solution developed for polyelectrolytes with low linear charge density.[6] The number of segments of the polymer is renormalized (reduced) as compared to the original polyelectrolyte, leading to an increased solubility. A trivial extension of this model to a multicomponent homopolymer solution gives (in our notation)

$$\beta(A - A^*) = -L \sum_x \frac{\phi_x}{r_x^{\text{eff}}} \ln \phi_x + \frac{L}{2} \sum_x \sum_{x'} \phi_x \chi_{xx'} \phi_{x'} \quad (8)$$

where the small ions now are *excluded* from the x and x' summations, and where the effective number of segments for the chain molecules is given by

$$r_x^{\text{eff}} = \frac{r_x}{1 + |\tau_x| r_x} \quad (9)$$

We will in the following refer to the model by Khokhlov and Nyrkova as the *effective length approximation*. Our treatment, where the counterions are treated explicitly, will be referred to as the *explicit counterions* approach.

The two approaches give different entropic and enthalpic contributions to the mixing free energy. This is easily demonstrated for the case of a polyelectrolyte solution without added salt. For the explicit counterions approach the free energy of mixing becomes according to eq 4

$$\frac{\beta(A - A^*)}{L} = -\left[\frac{\phi_p}{r_p} \ln \phi_p + \phi_c \ln \phi_c + \phi_s \ln \phi_s\right] + [\phi_p \chi_{pc} \phi_c + \phi_p \chi_{ps} \phi_s + \phi_c \chi_{cs} \phi_s] \quad (10)$$

whereas for the effective length approximation eqs 8 and 9 give

$$\frac{\beta(A - A^*)}{L} = -\left[\frac{\phi_p}{r_p} \ln \phi_p + |\tau_p| \phi_p \ln(\phi_p) + \phi_s \ln \phi_s\right] + [\phi_p \chi_{ps} \phi_s] \quad (11)$$

where the expressions in the two square brackets denote the entropic and enthalpic contributions, respectively, with ϕ_p, ϕ_c, and ϕ_s representing the volume fraction of polymers, counterions, and solvents, respectively. To proceed, we must address the difference in the treatment of the volume occupied by the counterions. Here, we have chosen to compare the results of the two approaches at the same volume fraction of the solvent. This implies that in the effective length approximation the volume occupied by the counterions (given by $\phi_c = |\tau_p|\phi_p$ in the explicit counterions approach) is absorbed in the volume of the polymer. Since $\phi_p + \phi_c = 1 - \phi_s$ in eq 10 and $\phi_p = 1 - \phi_s$ in eq 11, the meaning of ϕ_p is different in eqs 10 and 11, and the ϕ_p:s are related according to $\phi_p^{(\text{eq } 11)} = \phi_p^{(\text{eq } 10)}(1 + |\tau_p|)$. Thus, only the last entropic term, $\phi_s \ln \phi_s$, is identical, in the two free energy expressions. In regard to the enthalpy, two additional terms involving χ-parameters for the counterions appear in the explicit counterions approach. In the limit $\tau_x \to 0$, the two approaches trivially merge, since we then encounter a binary solvent/polymer system. However, the treatment with explicit counterions can also be used in the limit when one polyelectrolyte reduces to a simple salt (i.e., when $r_x = \tau_x = 1$). This fact is utilized below where we treat solvent/polyelectrolyte/salt mixtures by this approach.

Results and Discussion

Phase Behavior of Binary Solvent/Polymer Systems. We will first consider the effect of charging a polymer and including its accompanying counterions in the solution on the polymer solubility in binary solvent/polymer systems. Linear charge densities of the polyelectrolyte in the range $\tau_p = 0-0.7$ and chain lengths $r_p = 10$, 100, and 1000 have been employed. Figure 1 shows binodal curves and critical points for $r_p = 1000$ at indicated linear charge densities τ_p of the polymer. A system at specified $\phi_p + \phi_c$ and χ_{sp} separates into two phases above the binodal curve, whereas the system is monophasic below the binodal curve.[16]

For the uncharged polymer ($\tau_p = 0$), the numerically calculated coordinate of the critical point, $(\phi_{p,c}, \chi_{sp,c}) = (0.00307, 0.532)$ for $r_p = 1000$, agrees with the well-known analytic expression $(\phi_{p,c}, \chi_{sp,c}) = ((1 + \sqrt{r_p})^{-1}, (1 + 1/\sqrt{r_p})^2/2))$.[14] Also, for the polyelectrolyte systems the curves in Figure 1 are true binodal curves, since ϕ_p^α and ϕ_c^α are dependent through the electroneutrality condition (cf. the discussion of Figure 3 below when salt is added). It is clear from Figure 1 that the solubility of the polymer increases as it becomes more charged. Moreover, the introduction of the charges makes the

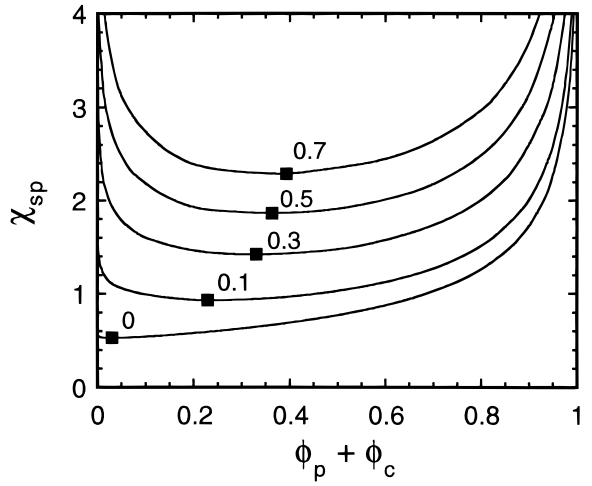

Figure 1. Phase diagram displaying binodal curves and critical points for the binary solvent/polymer system at $r_p = 1000$ and indicated linear charge density of the polymer τ_p. A system is biphasic above and monophasic below the binodal curves.

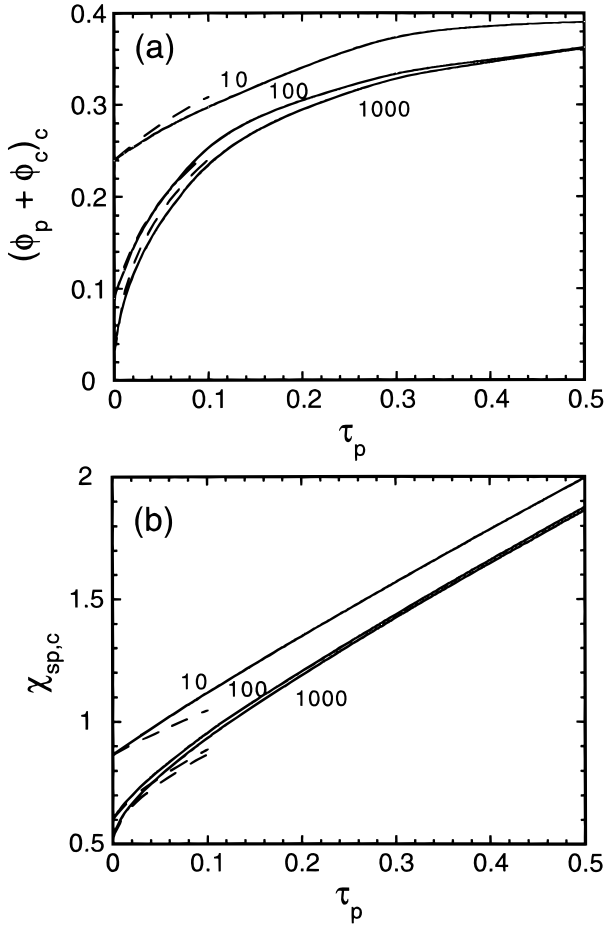

Figure 2. (a) Critical polyelectrolyte + counterion volume fraction $(\phi_p + \phi_c)_c$ and (b) critical interaction parameter $\chi_{ps,c}$ as a function of the linear charge density of the polyelectrolyte at indicated chain lengths (r_p) (solid curves). The corresponding results from the effective length approximation, eqs 8 and 9, are also given (dotted curves).

phase diagram more symmetric, displacing the critical points toward higher polymer concentrations. The changes are substantial: Already at $\tau_p = 0.1$ we notice that $(\phi_p + \phi_c)_c$ has increased to 0.23 and $\chi_{sp,c}$ becomes 0.934.

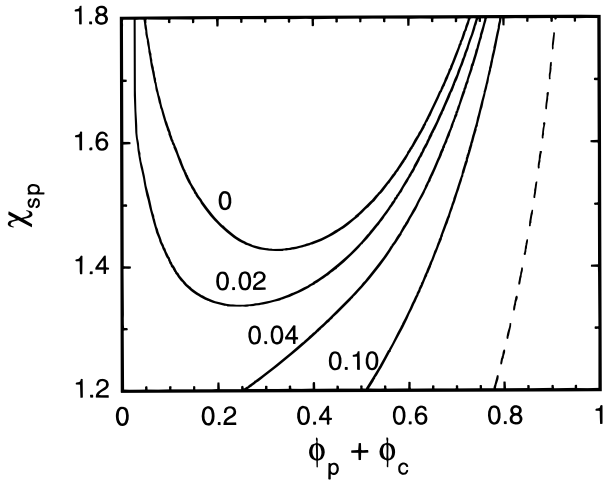

Figure 3. Partial phase diagram displaying coexisting curves for the ternary solvent/polyelectrolyte/salt system at $r_p = 1000$, $\tau_p = 0.3$, and indicated salt concentration ϕ_{salt} (solid curves) as obtained from an overall composition $\phi_p + \phi_c = 0.2$. The corresponding binodal curve for the solvent/polymer system without salt is also given (dashed curve).

Table 1. Critical Polyelectrolyte + Counterion Volume Fraction $(\phi_p + \phi_c)_c$ and Critical Interaction Parameter $\chi_{ps,c}$ for a Binary Solvent/Polyelectrolyte Solution at Different Chain Lengths (r_p) and Linear Charge Densities (τ_p)

	$r_p = 10$		$r_p = 100$		$r_p = 1000$	
τ_p	$(\phi_p + \phi_c)_c$	$\chi_{sp,c}$	$(\phi_p + \phi_c)_c$	$\chi_{sp,c}$	$(\phi_p + \phi_c)_c$	$\chi_{sp,c}$
0	0.24	0.866	0.09	0.605	0.031	0.532
0.1	0.30	1.12	0.27	0.955	0.23	0.934
0.3	0.38	1.57	0.34	1.44	0.33	1.43
0.5	0.39	2.00	0.36	1.88	0.36	1.87
0.7	0.39	2.41	0.39	2.30	0.39	2.29

As alluded to in the Introduction, the increased solubility of the polyelectrolyte is due to the presence of the dissolved counterions. Owing to the electroneutrality condition, there is a constraint on the distribution of the counterions between the phases. This additional constraint generally leads to an increase in the free energy for phase-separated systems relative to the homogeneous mixture. Thus, for polyelectrolyte systems the equilibrium between monophasic and biphasic states is shifted toward the monophasic one, and hence the extension of the biphasic region is reduced as compared to systems composed of uncharged polymers.

The values of $(\phi_p + \phi_c)$ and χ_{sp} at the critical point as a function of τ_p for the chain lengths $r_p = 10$, 100, and 1000 are given in Table 1. A subset of the data is displayed in Figure 2 (solid curves), where the predicted critical points from the effective length approximation are also given for small τ_p (dashed curves), where the approach is expected to be valid. For an uncharged polymer ($\tau_p = 0$), Figure 2 shows that $(\phi_p + \phi_c)_c$ and $\chi_{sp,c}$ are reduced with increasing r_p as predicted by the analytic expressions given above. At increasing linear charge density, $(\phi_p + \phi_c)_c$ and $\chi_{sp,c}$ increase for all r_p investigated. The increase is largest for large r_p, so for polyelectrolytes the critical $(\phi_p + \phi_c)$ and χ_{sp} display a smaller r_p-dependence as compared to those of uncharged polymers. In fact, Table 1 and Figure 2 show that, above some value of τ_p, which becomes smaller for larger r_p, $(\phi_p + \phi_c)_c$ is essentially r_p-independent. In the effective length approximation, this behavior may be seen directly from eq 9, which yields $r_p^{eff} = |\tau_p|^{-1}$ in the limit $|\tau_p| r_p \gg 1$.

Figure 2 also shows that the effective length approximation gives the correct results in the $\tau_p \rightarrow 0$ limit and accurately predicts the critical volume fractions and interaction parameters up to $\tau_p \approx 0.05-0.1$. At larger τ_p the effective length approximation underestimates $\chi_{sp,c}$ and the deviation of $(\phi_p + \phi_c)_c$ is less regular. The trend in $\chi_{sp,c}$ may be expected from the difference in the enthalpic contributions (eqs 10 and 11), given that the interaction parameters involving the counterions have been set to zero in our calculations. When τ_p is increased at a fixed total concentration of polyelectrolyte $(\phi_p + \phi_c)$, the volume of the counterions increases at the expense of the volume of the polymer molecules in the explicit counterions approach. This means that unfavorable polymer−solvent contacts are replaced by athermal counterion−solvent contacts. This dilution effect leads to a larger $\chi_{sp,c}$. In the effective length approximation, the enthalpy is insensitive to τ_p, since the volume of the counterions is neglected. This example also demonstrates that differences in the predicted phase diagrams of the two approaches depend on the choice of the two additional χ-parameters entering in the explicit counterions approach.

Phase Behavior of Ternary Solvent/Polymer/Salt Systems. It is well-known that it is possible to reduce the solubility of an intrinsically water-insoluble (hydrophobic) polyelectrolyte in water by adding sufficient amounts of salt. We will here treat this salting-out effect in a simple way, using the approach with explicit counterions. Figure 3 displays the boundaries between monophasic and biphasic regions for the chain length $r_p = 1000$ and the linear charge density $\tau_p = 0.3$ at different volume fractions of added monovalent salt (solid curves). The chemical nature of the counterions of the polyelectrolyte and of the salt is identical, and they are hence treated indistinguishably. The indicated volume fraction ϕ_{salt} denotes the sum of the volume fractions of the two ions of the monovalent salt. The phase boundary for the corresponding uncharged polymer without salt is also shown (dashed curve). For the charged polymer without added salt, and for the uncharged polymer, the calculated phase boundaries are binodal curves. However, for the polyelectrolyte with salt present, the phase boundaries are coexistence curves, since they depend on the overall composition of the system.[16] The solvent/salt composition of the two coexisting phases is a hidden variable in this simplified representation.

Figure 3 reveals that, at increasing concentrations of monovalent salt, the solubility of the polyelectrolyte is gradually reduced and the phase boundary is displaced toward that of the solvent/polymer system. However, even at the highest salt concentration, $\phi_{salt} = 0.10$ (well-above 1 M), there still remains a significant discrepancy between the coexistence curve of the ternary solvent/polyelectrolyte/salt system and the binodal curve of the binary solvent/polymer system (dashed curve). The magnitude of this difference is dependent again on the precise values of the interaction parameters for the small ions.

In Figure 4 we present partial ternary phase diagrams composed by binodal curves and tielines for the solvent/polyelectrolyte/salt close to the solvent/polyelectrolyte binary axis for three different values of χ_{sp}. Similar phase diagrams were obtained for $\tau_p = 0.1$ (data not shown). Besides the observation that salt reduces the solubility of the polyelectrolyte, Figure 4 also

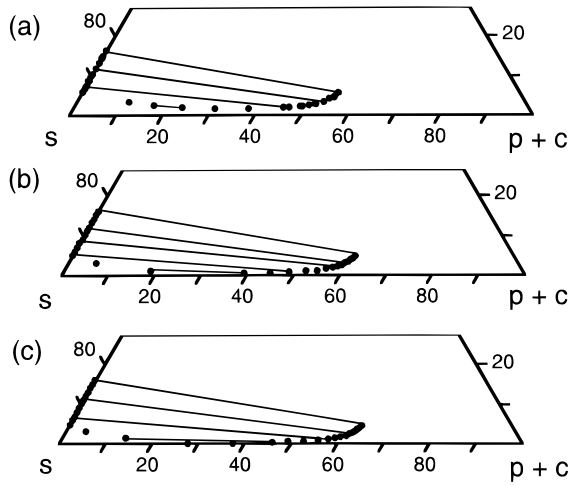

Figure 4. Phase diagrams displaying binodal curves (symbols) and tielines (lines) for a ternary solvent/polyelectrolyte/salt system close to the solvent/polyelectrolyte axis at $r_p = 1000$ and $\tau_p = 0.3$ with (a) $\chi_{sp} = 1.300$, (b) $\chi_{sp} = 1.390$, and (c) $\chi_{sp} = 1.426$.

demonstrates that the salt is unevenly distributed between the phases, the polyelectrolyte-poor phase being preferred. Considering the free energy contribution from the small ions and assuming that the entropic contribution dominates over the enthalpic, the explanation lies in the fact that the polyelectrolyte-rich phase already contains a considerable amount of counterions. Since the mixing entropy favors a distribution of the counterions as uniform as possible, the concentration of counterions in the polyelectrolyte-poor phase increases more than that in the polyelectrolyte-rich phase at the addition of salt. This tendency of an even counterion distribution is, however, counteracted by the mixing entropy of the coions, which is maximal at an *equal* coion concentration in the two phases. Hence, the actual distribution of the salt between the two phases is a compromise of the mixing entropy of the counterions and coions.

Phase Behavior of Ternary Solvent/Polymer 1/Polymer 2 Systems. The effects of charging one of the polymers in two different and strongly segregating ternary solvent/polymer 1/polymer 2 systems will be considered next. When uncharged, system I is symmetric with $\chi_{sp1} = \chi_{sp2} = 0.525$, $\chi_{p1p2} = 0.020$, and $r_{p1} = r_{p2} = 1000$. System II is specified by $\chi_{sp1} = 0.404$, $\chi_{sp2} = 0.525$, $\chi_{p1p2} = 0.020$, and $r_{p1} = r_{p2} = 1000$ and displays an asymmetry due to the different polymer−solvent interaction parameters. Related uncharged systems have been studied by Bergfeldt et al.[17] using the Flory−Huggins theory.

Figure 5 shows the ternary phase diagram for system I at indicated linear charge densities, τ_{p1}, of polymer 1 with polymer 2 uncharged, $\tau_{p2} = 0$. The binodal curves given by the effective length approximation are also included (symbols). We have monophasic regions above the indicated binodal curves toward the solvent corner, and the tielines in the biphasic regions indicate the composition of the coexisting phases. There is a very good agreement between effective length approximation and the treatment with explicit counterions.

For uncharged polymer 1, $\tau_{p1} = 0$, we indeed obtain a symmetric binodal curve and the extension of the monophasic region is small since the miscibility of the two polymers is low. At a successively higher linear charge density of polymer 1, the miscibility of the

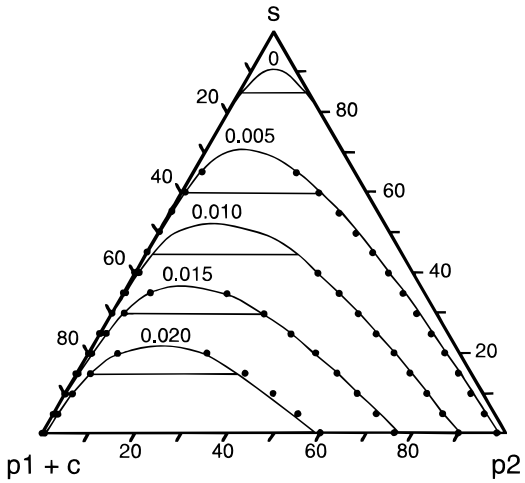

Figure 5. Phase diagram displaying binodal curves (solid curves) and tielines (lines) for ternary solvent/polymer 1/polymer 2 systems (system I) with $\tau_{p2} = 0$ at the indicated linear charge density of polymer 1, τ_{p1}. The binodal curves from the effective length approximation are also given (symbols).

polymers increases, and a complete miscibility is obtained at a linear charge density of $\tau_{p1} \approx 0.03$. At the same time, the phase diagram becomes increasingly asymmetric with the biphasic region displaced toward the solvent/polymer 1 binary axis. The tielines are nearly parallel to the polymer 1−polymer 2 axis; thus, the volume fractions of the solvents approximately equal in the coexisting phases.

The reduced extension of the biphasic region upon charging one of the polymers can again be explained by invoking the effect of the mixing entropy of the counterions. The arguments are the same as for the binary system; the difference is merely that the phase separation in the ternary system is driven by the repulsive polymer 1−polymer 2 interaction. Furthermore, the asymmetric appearance of the binodal is a consequence of the tendency of having an equal counterion concentration (and a concomitant equal distribution of the charged polymers) in the two coexisting phases. For example, consider the overall composition $\phi_s = 0.2$ and $\phi_{p1} = \phi_{p2} = 0.4$. For uncharged polymer 1, we have $\phi^1_{p1}/\phi^2_{p1} > 100$. For $\tau_{p1} = 0.015$, this ratio is reduced to $\phi^1_{p1}/\phi^2_{p1} \approx 2.4$, whereas polymer 2 still remains unevenly distributed between the two phases: $\phi^1_{p2}/\phi^2_{p2} \approx 1/25$.

Figure 6 shows the relationship between τ_{p1} and the maximum χ_{p1p2} for complete miscibility in more detail. The condition for complete miscibility is described by a nearly linear relation between τ_{p1} and χ_{p1p2}. Hence, in systems with unfavorable polymer−polymer interactions and low miscibility, we can increase the miscibility by introducing charges on one of the polymers. An increased miscibility in aqueous polymer/polymer mixtures upon charging one of the polymer components has been also observed experimentally, for example, by Vasilevskaya et al.,[1] Iliopoulos et al.,[2] and Bergfeldt et al.[5] Khokhlov and Nyrkova have previously shown[6] that the effective length approximation predicts a behavior in qualitative agreement with that of the system investigated by Vasilevskaya et al.

Phase diagrams for system II at different linear charge densities of polymer 1 with polymer 2 uncharged are given in Figure 7. For uncharged polymer 1, the asymmetry of the phase diagram is strong. The condition $\chi_{sp1} < \chi_{sp2}$ leads to a relatively more concentrated

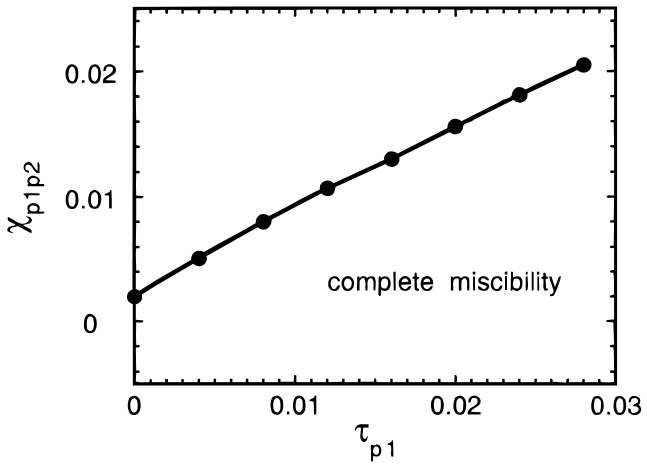

Figure 6. Boarder of the region of complete miscibility for system I in the (τ_{p1}, χ_{p1p2})-space (symbols, the curve is only a guide for the eye).

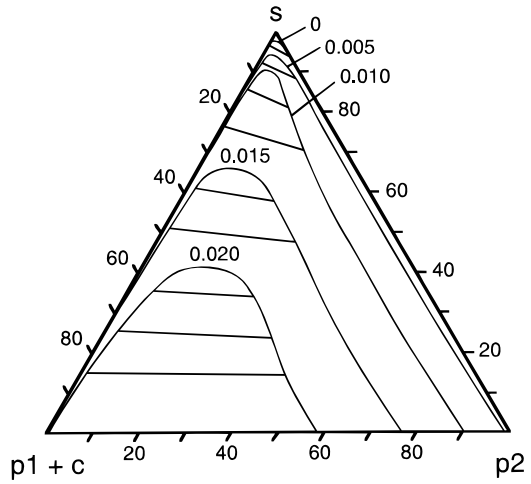

Figure 7. Phase diagram displaying binodal curves and tielines for ternary solvent/polymer 1/polymer 2 systems (system II) with $\tau_{p2} = 0$ at the indicated linear charge density of polymer 1, τ_{p1}.

polymer 2-rich phase and a relatively more dilute polymer 1-rich phase as shown by the tilted tieline (the uppermost solid line).

As for system I, the effect of charging one of the polymers in the asymmetric system II leads to a decrease of the biphasic region ending with a complete miscibility at a sufficiently large charge density. The value of τ_{p1} required for complete miscibility is comparable to that for system I. Also in system II, the binodal curve is displaced toward the solvent/polymer 1 binary axis at increasing τ_{p1}. Moreover, at increasing τ_{p1} the tielines become more parallel to the polymer 1/polymer 2 binary axis, thus expressing a more even distribution of the solvent between the two coexisting phases. Hence, an unequal distribution of the solvent between the phases due to different solvency can be compensated for by introducing charges on the most soluble polymer. A similar appearance is also expected when charging up the least soluble polymer.

We will now investigate the phase behavior at different linear charge densities of one of the polymers when the other polymer carries a fixed number of charges. Starting from system II, we assign a fixed linear charge density $\tau_{p1} = 0.010$ to the more soluble polymer, whereas the linear charge density of the less soluble polymer

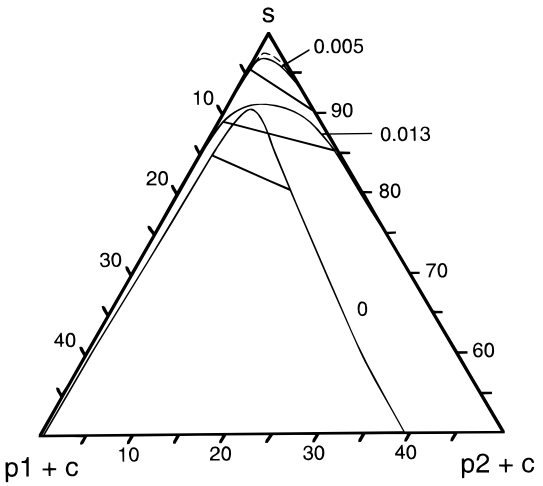

Figure 8. Phase diagram displaying binodal curves and tielines for ternary solvent/polymer 1/polymer 2 systems (system II) with $\tau_{p1} = 0.010$ at the indicated linear charge density of polymer 2, τ_{p2}. The binodal curve for system II with $\tau_{p1} = \tau_{p2} = 0$ is also given (dashed curve).

varies from $\tau_{p2} = 0$ to 0.020. Figure 8 shows the obtained phase diagrams for $\tau_{p2} = 0$, 0.005, and 0.013. At the intermediate linear charge density, the system displays the largest biphasic region. At both larger and smaller linear charge densities of polymer 2, the extension of the biphasic region is reduced and the tielines become less tilted. Hence, there exists a value of τ_{p2} at which the miscibility has a minimum.

Figure 9a shows more clearly the variation in the extension of the biphasic region by displaying the sum of the polymer and counterion volume fractions at the critical point, $(\phi_{p1} + \phi_{p2} + \phi_c)_c$, as a function of τ_{p2} for two different values of τ_{p1}. For $\tau_{p1} = 0.010$, the miscibility goes through a minimum at $\tau_{p2} \approx 0.005$. Thus, the minimum is not situated at an equal linear charge density of the two polyelectrolytes, but rather at a point determined by both the linear charge densities and the interaction parameters. The phase diagram at the minimum resembles very much the phase diagram of the uncharged system (cf. the dashed curve and the curve labeled 0.005 in Figure 8). A comparison of data for $\tau_{p1} = 0.010$ and 0.015 in Figure 9a shows that the minimum of $(\phi_{p1} + \phi_{p2} + \phi_c)_c$ is displaced to higher τ_{p2} and becomes shallower as τ_{p1} is increased.

As mentioned in the Introduction, experimental phase studies of segregating pseudo ternary water/polyelectrolyte/charged micelle systems have been performed by Bergfeldt and Piculell.[5] They used sodium dextran sulfate (DxS), with different low degrees of sulfation, mixed with penta(ethylene oxide) dodecyl ether ($C_{12}E_5$), to which sodium dodecyl sulfate (SDS) was added to obtain micelles with an adjustable charge. Most interestingly, they found that with charged dextran the miscibility first decreased and then increased upon increasing the micellar charge. In Figure 9b we reproduce their results for DxS with 2.5% of the sugar groups negatively charged at a polymer-to-surfactant weight ratio of 7:3. The experiment is in line with the calculations of Figure 9a, showing the total concentration of the polymer and surfactant at the phase boundary (close to the critical point) at an increasing mole fraction of SDS of the surfactant. There is a good qualitative agreement between theory and experiment, with a minimum occurring in the experimental mixtures when the mole fraction of SDS is increased from 0 to 0.13.

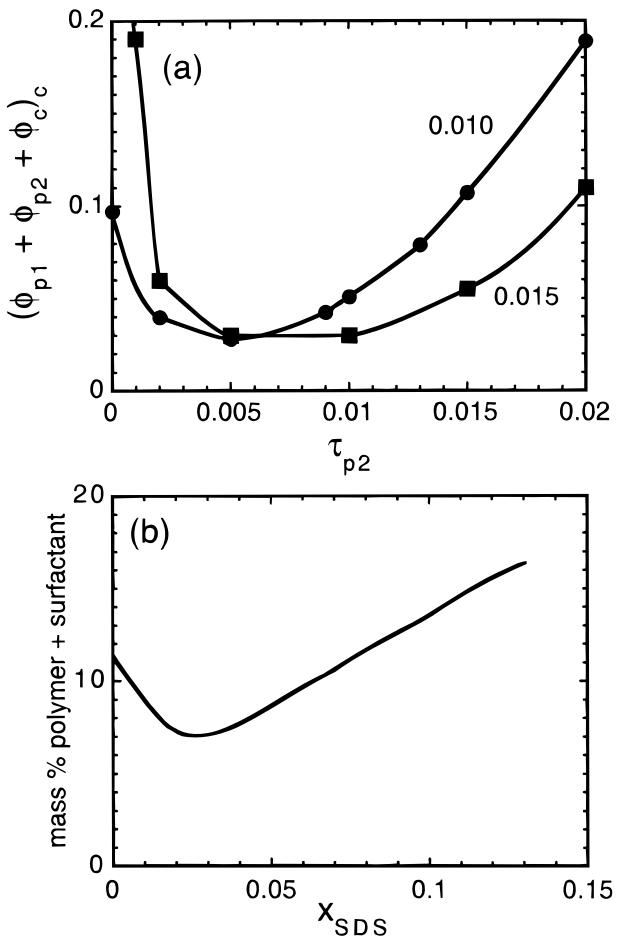

Figure 9. (a) Sum of the volume fractions of polymers 1 and 2 at the critical point $(\phi_{p1} + \phi_{p2})_c$ for system II at the indicated τ_{p1} as a function of τ_{p2} (symbols, the curve is only a guide for the eye). (b) Total concentration of polymer + surfactant at the phase boundary as a function of the mole fraction of SDS of the surfactant in mixtures with dextran sulfate with 2.5% of the sugar groups charged. Further details are given in the text. Data taken from ref 5.

The experiments in ref 5 also display that τ_{p2} at the minimum becomes larger and the minimum becomes shallower at increasing τ_{p1}, as predicted in Figure 9a. Thus, as the charge of the two polyelectrolytes is increased, the phase diagram of their mixture becomes less sensitive to small changes in charge density of one of the components around the minimum in the miscibility.

The similarity of the theoretical and experimental data in Figure 9 supports the conclusion by Bergfeldt and Piculell that the variation of the extension of the phase diagrams in ref 5 is primarily an effect of the counterions of the charged polymers arising from the requirement that each phase has to be electroneutral.

From previous model calculations[4] it was proposed that the largest extension of the biphasic region would be achieved for such charge densities of the macroions that the same counterion concentration is obtained in both phases. This conclusion was later supported by experimental investigations.[5] To further examine this point, we have calculated the difference of the volume fraction of the counterions between the two coexisting phases from the system given in Figure 8. More precisely, we have considered the partial derivative of the difference in the volume fraction of the counterions between the coexisting phases ($\Delta\phi_c$) with respect to the

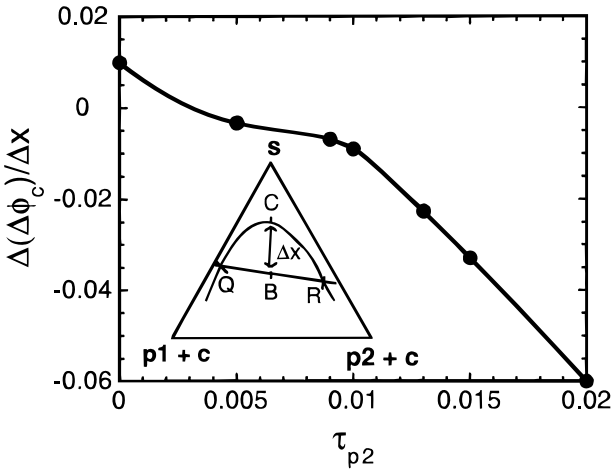

Figure 10. The partial derivative $(\partial\Delta\phi_c/\partial_x)_{x=0}$ for system II with $\tau_{p1} = 0.010$ as a function of τ_{p2} (symbols, the curve is only a guide for the eye). The ordinate is approximated as $(\partial\Delta\phi_c/\partial_x)_{x=0} \approx \Delta(\Delta\phi_c)/\Delta x = (\Delta\phi_{c,B} - \Delta\phi_{c,C})/(x_B - x_C) = (\phi_{c,Q} - \phi_{c,R})/(x_B - x_C)$, where $\Delta\phi_{c,C} \equiv 0$ by definition. Points *B*, *Q*, and *R* are defined in the insert, *B* is the midpoint of *QR*, and the points *Q* and *R* were chosen so that $\phi_{p1,B} - \phi_{p1,C} \approx 0.02$.

"distance" (x) between the overall composition of the system and the composition at the critical point in the limit $x \rightarrow 0$ (i.e., $(\partial\Delta\phi_c/\partial_x)_{x=0}$). Further explanation of the quantity $(\partial\Delta\phi_c/\partial_x)_{x=0}$ is given in Figure 10.

Figure 10 shows that $(\partial\Delta\phi_c/\partial_x)_{x=0} > 0$ at $\tau_{p2} = 0$ and < 0 at $\tau_{p2} = 0.020$, with a continuous decrease in between. Hence, at $\tau_{p2} = 0$ the polyelectrolyte 1-rich phase has a larger counterion concentration, whereas the opposite is the case at large τ_{p2}. The zero crossing appears at $\tau_{p2} \approx 0.003$ which, indeed, is close to the linear charge density where the biphasic region has its largest extension. However, there is not a complete matching. Thus, there is an influence of higher order factors to the condition for minimum miscibility. This is evident also from the fact that the minimal slope of $(\partial\Delta\phi_c/\partial_x)_{x=0}$ versus τ_{p2} appears at $(\partial\Delta\phi_c/\partial_x)_{x=0}$ slightly off zero (see Figure 10).

Charged Poly(propylene oxide) and Poly(ethylene oxide) Systems. The Flory–Huggins lattice theory for homogeneous polymer solutions has been extended to polymers possessing internal states.[10] The basis of the polymer model is that the distribution of conformations of a segment depends on temperature, and that different conformations interact differently with adjacent polymer segments and solvent molecules. The conformations of the OCCO segment of PEO are divided into two classes or states, one being polar and having a low energy but a low statistical weight, and one being less polar, or nonpolar, having a higher energy but a higher statistical weight. At a low temperature the former state is dominating, and thus a more favorable polymer–water interaction is obtained, whereas at elevated temperatures, the latter state becomes progressively more important, resulting in a more unfavorable polymer–water interaction. Hence, this approach leads to effective segment–segment interaction parameters which depends on both temperature and concentration by utilizing a physical model. Furthermore, the approach has proved to be very fruitful for modeling the self-association,[11] the phase behavior,[12] and the adsorption at interfaces[13] of ethylene oxide (EO) and propylene oxide (PO) containing block copolymers.

By including electrostatic effects, we will be able to make predictions of the phase behavior of charged polymers containing EO and PO segments. In the following we present results of the phase behavior of the binary water/PPO and the binary water/PO–EO random copolymer and how the solubility changes when the polymers are charged using such an approach. To the best of our knowledge, such systems have not yet been investigated experimentally. All relevant parameters for the modeling of the homopolymers and copolymers containing EO and PO are given in Table 2. These parameters have previously been obtained by fitting calculated phase diagrams of simple systems containing water, EO, and PO[10,15,18,19] and they have been extensively used to model EO- and PO-containing polymers.

Table 2. Internal State Parameters (U_{AB} and g_{AB}) and Flory–Huggins Interaction Parameters ($\chi_{BB'}$) of the Theoretical Model (Energy in kJ mol^{-1})

species	state	U_{AB}	g_{AB}
water		0	1
EO	polar	0	1
	nonpolar	5.086[a]	8[a]
PO	polar	0	1
	nonpolar	11.5[b]	60[b]

	$RT\chi_{BB'}$			
	EO(polar)	EO(nonpolar)	PO(polar)	PO(nonpolar)
water	0.6508[a]	5.568[a]	1.7[b]	8.5[b]
EO(polar)		1.266[a]	1.8[c]	3.0[c]
EO(nonpolar)			0.5[c]	−2.0[c]
PO(polar)				1.4[b]

[a] From the fit to the experimental data of the binary PEO/water phase diagram (see refs 9 and 18). [b] From the fit to the experimental data of the binary PPO/water phase diagram (see ref 15). [c] From the fit to the experimental data of the ternary PEO/PPO/water phase diagram (see ref 19).

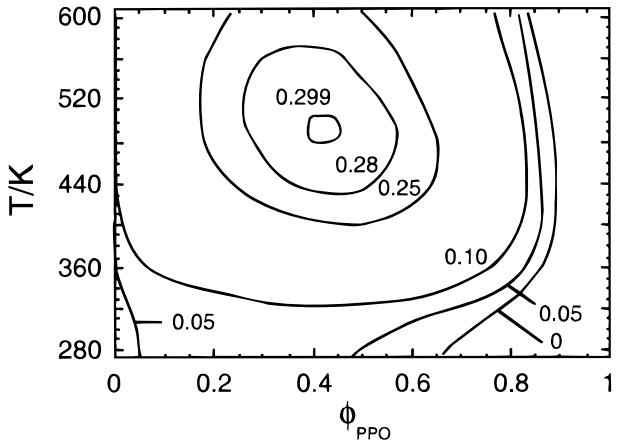

Figure 11. Phase diagrams for binary water/PO_{1000} systems at the indicated linear charge density of the PO_{1000}. Interaction parameters according to Table 2.

Uncharged PPO is virtually insoluble in water except at a very low molecular mass. On the basis of the previous results, we anticipate that by introducing charges the solubility of PPO in water increases. Figure 11 shows the phase diagram of the binary water/PO_{1000} system where τ_{PO} varies between 0 and 0.299. The regions above the binodal curves, or within them if they are closed loops, are the biphasic areas. It is thus seen that the solubility of PO_{1000} indeed increases with its linear charge density, and at sufficiently high τ_{PO}, PO_{1000} becomes soluble at all temperatures and concentrations. The dependence of the lower critical point (T_c) on τ_{PO} for different chain lengths is displayed in Figure 12. We see a continuous rise in T_c with τ_{PO} and this increase is

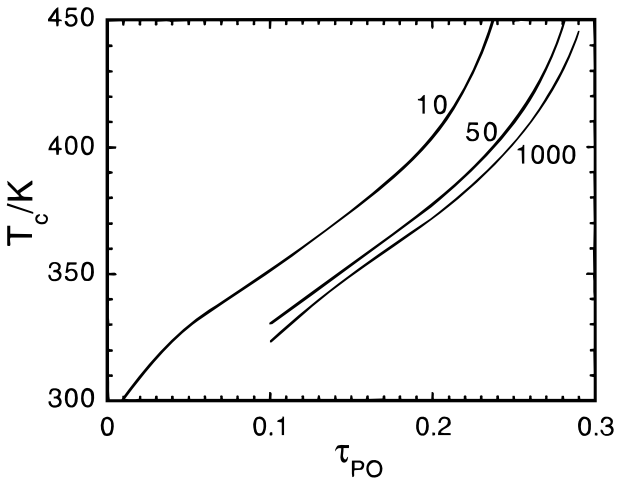

Figure 12. Lower critical temperature (T_c) for the binary water/PPO system as a function of the linear charge density τ_{PO} at the indicated chain length r_{PPO}.

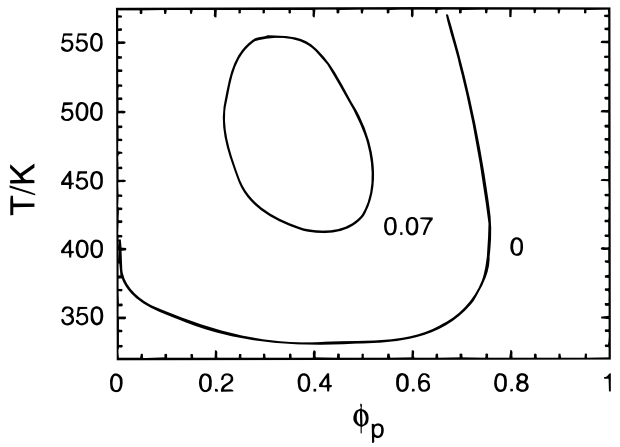

Figure 13. Phase diagrams for binary water/random $EO_{42}PO_{14}$ systems at the indicated linear charge density of the copolymer. Interaction parameters according to Table 2.

essentially independent of the chain length except for a temperature shift.

The solubility of PPO can be increased by replacing PO monomers by EO monomers which have a higher solubility. By such means, the solubility and the lower critical temperature of the polymer can be tuned. Random copolymers composed by EO and PO are commercially available.

We have investigated the phase diagrams for a number of EO/PO random copolymers. Figure 13 shows the phase diagram for the binary water/$EO_{42}PO_{14}$ system at $\tau_p = 0$ and 0.07. Again we see that the solubility of the polymer is increased as the polymer is charged. These calculations suggest that, besides the EO/PO balance, also the introduction of charges may be a tool for tuning the solubility of these copolymers. Whereas the solubility of the uncharged polymers is insensitive of the salt concentration, the solubility of the charged modified polymers is sensitive to the salt concentration which hence could be employed. For example, instead of inducing phase separation by a temperature increase, a similar phase change could be induced by adding salt.

To conclude, the favorable miscibility enhancement upon charging the polymers found in the more generic investigations reappears and this could possibly be exploited to control the solubility of alkoxy polymers.

Summary

On the basis of an extension of the Flory−Huggins lattice theory for homogeneous polymer solutions, we have investigated the change of the solubility by introducing charges on the polymers and counterions in the solution. The extension of the previous lattice theory involved the explicit inclusion of the counterions and any potential salt components in the model on an equal footing as the solvent and the polymeric components. The effect of the electrostatic interaction among the charges was treated as simple as possible—a requirement that all phases have to be electroneutral. Hence, there were no explicit terms describing the electrostatic energy contribution to the free energy of the system.

With this simple approach we have shown the following:

(1) The solubility of a polymer in a solvent increases as the polymer is charged.

(2) In the same system, the solubility of the charged polymer is reduced upon the addition of salt.

(3) The biphasic region of ternary solvent/polymer/polymer systems is reduced as one of the polymers is charged.

(4) The extension of the biphasic region for charged ternary solvent/polymer/polymer systems depends on the solvencies and linear charge densities of the polymers. At the maximal extension of the biphasic region, the linear charge densities of the two polymers should match any differences in the polymer solvencies such that the concentrations of the counterions are approximately equal in the two coexisting phases.

(5) The solvency of the commercially important alkoxy polymers may be adjusted by introducing charged groups.

(6) The effective length approach by Khokhlov and Nyrkova, which is an approximation to the present approach, works excellently for polyelectrolytes with linear charge densities up to approximately $\tau \approx 0.05-0.10$.

(7) There is a qualitative agreement on points (1)−(4) between experimental results and our predictions, suggesting that the counterion mixing entropy is the main factor controlling the difference in the phase behavior between noncharged and charged polymers in real systems. However, this does not exclude that further extensions of the theory where the electrostatic interactions within the phases are explicitly taken into account, by for example the Poisson−Boltzmann equation, is important for further progress.

Finally, for different systems we have seen that polyelectrolytes display a larger solubility than the corresponding neutral polymers. The reason is associated with the counterions of the polyelectrolyte. The addition of counterions to the system reduces the free energy of the one-phase system more than that of the two-phase system. In the one-phase system the counterions maximize their mixing entropy by being evenly distributed, whereas in the two-phase system their mixing entropy is smaller due to their uneven distribution between the phases caused by the electroneutrality constraint applied to the phases separately.

Acknowledgment. This work was supported by the Swedish National Science Research Council (NFR) and the Swedish Research Council for Engineering Sciences (TFR).

References and Notes

(1) Vasilevskaya, V. V.; Starodoubtsev, S. G.; Khokhlov, A. R. *Vysokomolec. Soed.* **1987**, *29B*, 390.
(2) Iliopoulos, I.; Frugier, D.; Audebert, R. *Polym. Prepr. (Am. Chem. Soc., Div. Polym. Chem.)* **1989**, *30*, 371.
(3) Piculell, L.; Nilsson, S.; Falck, L.; Tjerneld, F. *Polym. Commun.* **1991**, *32*, 158.
(4) Piculell, L.; Ilioupolos, I.; Linse, P.; Nilsson, S.; Turquois, T.; Viebke, C.; Zhang, W. *Gums and Stabililisers for the Food Industry*; Oxford University Press: Oxford, 1994; Vol. 7, p 309.
(5) Bergfeldt, K.; Piculell, L. *J. Phys. Chem.* **1996**, *100*, 5935.
(6) Khokhlov, A. R.; Nyrkova, I. A. *Macromolecules* **1992**, *25*, 1493.
(7) Piculell, L.; Lindman, B. *Adv. Colloid Interface Sci.* Elsevier Science Publishers B. V.: Amsterdam, 1992; Vol. 41, p 149.
(8) Johansson, H.-O.; Karlström, G.; Mattiasson, B.; Tjerneld, F. *Bioseparation* **1995**, *5*, 269.
(9) Piculell, L.; Bergfeldt, K.; Gerdes, S. *J. Phys. Chem.* **1996**, *100*, 3675.
(10) Karlström, G. *J. Phys. Chem.* **1985**, *89*, 4962.
(11) Linse, P. *Macromolecules* **1993**, *26*, 4437.
(12) Noolandi, J.; Shi, A.-C.; Linse, P. *Macromolecules* **1996**, *29*, 5907.
(13) Linse, P.; Hatton, T. A. *Langmuir* **1997**, *15*, 44066.
(14) Flory, P. J. *Principles of Polymer Chemistry*; Cornell University Press: Ithaca, NY, 1953.
(15) Linse, P.; Björling, M. *Macromolecules* **1991**, *24*, 6700.
(16) For a discussion on the differences between binodal curves and coexistence curves in multicomponent systems, see Chapter 8 (and references therein) of Fujita, H. *Polym. Solutions*; Elsevier Science Publishers B. V.: Amsterdam, 1990.
(17) Bergfeldt, K.; Piculell, L.; Linse, P. *J. Phys. Chem.* **1996**, *100*, 3860.
(18) Björling, M.; Linse, P.; Karlström, G. *J. Phys. Chem.***1990**, *94*, 471.
(19) Malmsten, M.; Linse, P.; Zhang, K.-W. *Macromolecules* **1993**, *26*, 2905.

MA980866D